10.6 MICRON PARAMETRIC FREQUENCY CONVERTER

R. L. Abrams

Hughes Research Laboratories

Prepared for:

Office of Naval Research
Advanced Research Projects Agency

March 1975

UNCLASSIFIED

SECURITY CLASSIFICATION OF THIS PAGE (When Data Entered)

REPORT DOCUMENTATION PAGE		READ INSTRUCTIONS BEFORE COMPLETING FORM
1. REPORT NUMBER	2. GOVT ACCESSION NO.	3. RECIPIENT'S CATALOG NUMBER AD-A009 112
4. TITLE (and Subtitle) 10.6 MICRON PARAMETRIC FREQUENCY CONVERTER		5. TYPE OF REPORT & PERIOD COVERED Semiannual Tech. Report 1 Sept. 1974-28 Feb. 1975 6. PERFORMING ORG. REPORT NUMBER
7. AUTHOR(s) R.L. Abrams		8. CONTRACT OR GRANT NUMBER(s) N00014-75-C-0089
9. PERFORMING ORGANIZATION NAME AND ADDRESS Hughes Research Laboratories 3011 Malibu Canyon Road Malibu, California 90265		10. PROGRAM ELEMENT, PROJECT, TASK AREA & WORK UNIT NUMBERS ARPA Order No. 1806
11. CONTROLLING OFFICE NAME AND ADDRESS Advanced Research Projects Agency 1400 Wilson Boulevard Arlington, Virginia 22209		12. REPORT DATE March 1975 13. NUMBER OF PAGES 34
14. MONITORING AGENCY NAME & ADDRESS(if different from Controlling Office) Office of Naval Research 800 No. Quincy Street Arlington, Virginia 22217		15. SECURITY CLASS. (of this report) Unclassified 15a. DECLASSIFICATION DOWNGRADING SCHEDULE
16. DISTRIBUTION STATEMENT (of this Report)		
17. DISTRIBUTION STATEMENT (of the abstract entered in Block 20, if different from Report)		
18. SUPPLEMENTARY NOTES		
19. KEY WORDS (Continue on reverse side if necessary and identify by block number) CO_2 Laser Nonlinear Mixing Frequency Conversion Tunable Laser		PRICES SUBJECT TO CHANGE

20. ABSTRACT (Continue on reverse side if necessary and identify by block number)

This program represents an effort to demonstrate nonlinear mixing induced in a molecular gas by the application of a dc electric field. In particular, the molecule NH_2D is considered as a three level system interacting simultaneously with applied infrared and microwave radiation. The molecular energy levels are tuned via the Stark effects such that the three levels are simultaneously resonant with the applied frequencies ω_2 and ω_3. A resonant nonlinear interaction occurs

DD FORM 1 JAN 73 1473 EDITION OF 1 NOV 65 IS OBSOLETE

UNCLASSIFIED

SECURITY CLASSIFICATION OF THIS PAGE (When Data Entered)

resulting in the generation of a third frequency at $\omega_1 = \omega_3 - \omega_2$. This process is allowed due to the removal of inversion degeneracy in the gas by the applied field.

The theory of the three level system interacting with two applied fields is treated in the general case where both dopplier and collision broadening are important. The nonlinear coefficient is related to measured parameters such as the Stark tuning rate and the optical linear absorption coefficient. It is shown that the effective resonant electro-optic coefficient for mixing of 10.6 μm radiation with 4.1 GHz microwaves in NH_2D is comparable to the value in single crystal GaAs, one of the best electro-optic materials available. The modulation process results in single sideband generation, in contrast to most modulation schemes. The dispersion in the nonlinear coefficient is also calculated, showing that it becomes complex for the nonresonant case, with the imaginary part several times larger than the value of the real part on resonance.

Experimental apparatus has been assembled and tested for a laboratory measurement of the phenomenon. A Stark cell has been constructed which allows simultaneous application of dc and rf fields as well as transmission of 10.6 μm radiation. Problems with vacuum integrity and RFI have thus far prevented the observation of the single sideband modulation. Improvements in rf shielding and redesign of the vacuum enclosure should allow observation of the predicted effect.

ARPA Order No.	1806
Program Code Number	5E20
Effective Date of Contract	1 September 1974
Contract Expiration Date	31 August 1975
Amount of Contract	$99,958.00
Principal Investigator	R.L. Abrams (213) 456-6411 ext. 498
Scientific Officer	Director, Physics Program Physical Sciences Division Office of Naval Research 800 North Quincy Street Arlington, Virginia 22217

This research was supported by the Advanced Research Projects Agency of the Department of Defense and was monitored by ONR under Contract No. N00014-75-C-0089.

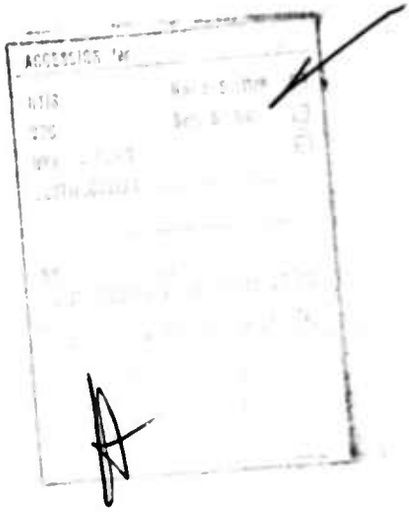

FOREWORD

The following personnel contributed to the research reported here: Prof. Amnon Yariv, a consultant to Hughes Research Laboratories, P. Yeh, and R.L. Abrams contributed to the theoretical treatment of the nonlinear interaction. The microwave Stark Cell development and optical measurements were made by A. Popa, with the technical assistance of R. Niedziejko and R. Brower.

TABLE OF CONTENTS

I. INTRODUCTION AND SUMMARY

A. Background

It is anticipated that modern optical radar systems for surveillance of orbiting objects will require new types of electro-optical devices capable of frequency control and frequency conversion of infrared laser radiation. This program addresses an approach which should lead to a new class of electro-optical devices such as single sideband modulators, tunable local oscillators, and frequency shifters, using the resonant interaction of optical and microwave fields in a gas whose energy level structure is controlled by an applied electric field (Stark effect).

The molecule NH_2D has an infrared absorption line which may be tuned into resonance with the P(20) 10.6 μm CO_2 laser transition by application of an electric field. This transition has been studied extensively[1,2] and has been used to intensity modulate the CO_2 laser at low frequencies.[3] More recently, at Hughes Research Laboratories, we have exploited this interaction to frequency stabilize a gigahertz tunable waveguide CO_2 laser,[4] demonstrating precise control of the waveguide laser frequency over a bandwidth greater than 1 GHz, and solving one of the major problems in CO_2 laser frequency control. The experience with these interactions in Stark tunable molecules has stimulated the concepts and ideas which are being implemented in this program.

B. Basic Concept

The energy level scheme for NH_2D is more thoroughly discussed in Section II of this report. In order to illustrate the basic mechanism for the interaction, consider the simplified energy level diagram shown in Fig. 1. Upon application of an electric field (of appropriate magnitude), two NH_2D energy levels, labeled 1 and 3 in Fig. 1, will become resonant with the laser frequency. A third level (level 2) is also tuned

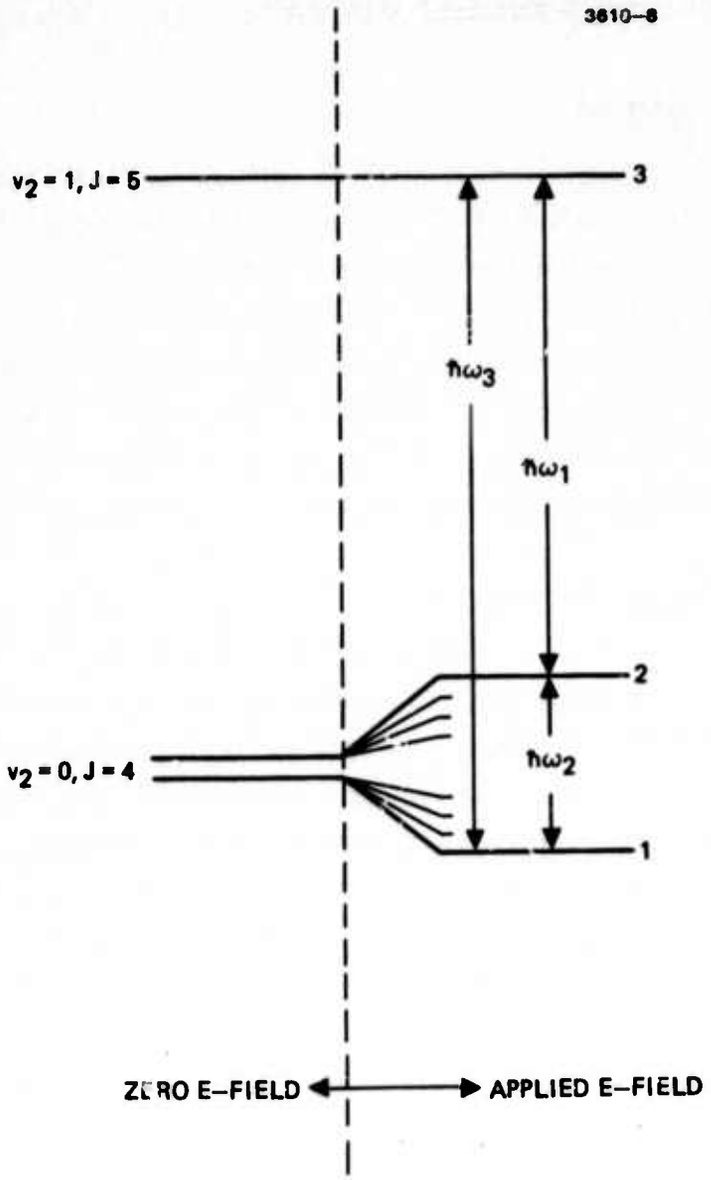

Fig. 1. Simplified energy level diagram for NH_2D, showing relevant levels in an applied electric field. The P(20) 10.6 μm radiation is incident at frequency ω_3, ω_2 is the applied microwave frequency, and ω_1 is the newly generated sideband frequency.

by the electric field. The key element of this system is that the applied field breaks inversion symmetry and induces a permanent dipole moment. The three electric dipole moments μ_{12}, μ_{13}, μ_{23} are all non-zero, due to the applied electric field, and this allows us to consider a number of possible strong interactions which would ordinarily be very weak. The proposed experiment involves the simultaneous application of two fields to the NH_2D, an applied field at ω_3 (the CO_2 laser resonant with levels 1 and 3), and an rf signal at ω_2 (resonant with levels 1 and 2 at ~4.1 GHz). Quantum mechanical calculations, discussed in Section II, show that it is possible to generate a signal at $\omega_1 = \omega_3 - \omega_2$, and that measurable conversion efficiency is possible with modest amounts of rf power. This surprising result is largely due to the nonvanishing dipole matrix elements induced by the applied field. In effect, the gas becomes the vehicle for a field induced resonant nonlinear interaction.

C. Progress

Section II contains a summary of our progress on the theory of the nonlinear interaction. The resonant nonlinear coefficient is derived for stationary molecules (no doppler broadening) and the result is then integrated over the molecular velocity distribution, esulting in a general expression for arbitrary amounts of doppler and pressure broadening. The result is then extended for off resonance operation, and it is shown that the nonlinear coefficient becomes complex, with the imaginary part displaying a magnitude considerably larger than the real part. This may be important in finding means to extend the bandwidth of the effect. The value of the coefficient is related to the high pressure limiting value of the linear absorption coefficient resulting in a simple expression for accurately estimating its magnitude. A resonant value of

$$d^{\omega_1 = \omega_3 - \omega_2} = 9.6 \times 10^{-8} \text{ esu}$$

is calculated, but this may be enhanced by a factor of 3 to 4 by off resonance operation.

Progress on the experimental aspects of the program is discussed in Section III. Most of the effort to date has involved design and testing of microwave Stark cell structures. A triplate transmission line has been built and tested. Q values as high as 250 at 4.1 GHz have been measured with simultaneous application of dc and microwave fields. Reliable vacuum sealing of this device has been difficult, however. A second structure, originally designed for low frequency Stark cell measurements has proven to be usable at frequencies up to 100 MHz. This device is now being modified to operate at 4.1 GHz, and has the advantage that the entire structure is contained in a metal cylinder, providing excellent rf containment. Both structures are being refined for future measurements.

D. Plans

During the second half of the program, the emphasis will be placed on an experimental demonstration of the predicted nonlinear effect. The additional analysis to be performed consists of a prediction of the saturation behavior of the nonlinear coefficient with increasing rf and optical power densities. Experimentally, the two types of microwave Stark cells will be completed and evaluated and a concentrated effort will be made to observe the predicted signals. Detailed comparisons with the theoretical predictions will then be made.

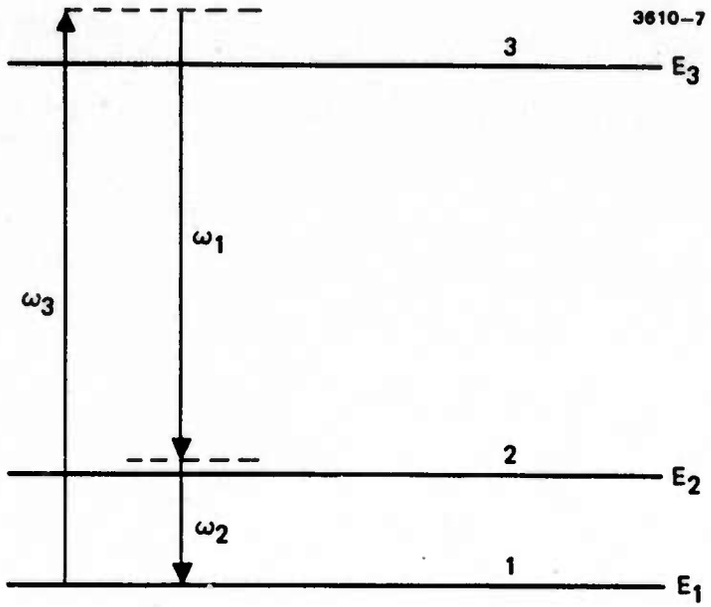

Fig. 2. Three-level system used in deriving the nonlinear optical coefficient.

We apply the density matrix formalism. The α component of the polarization is given by

$$P_\alpha = N\mathrm{tr}\,(\rho\mu_\alpha) \tag{1}$$

where N is the density of molecules, ρ the density matrix, and $\vec{\mu}$ the dipole moment operator. tr stands for the trace (sum of diagonal terms).

The system Hamiltonian is taken as

$$= H_o + V = H_o - \vec{\mu} \cdot \vec{E}(t) \tag{2}$$

where $\vec{E}(t)$ is the applied oscillating electric field. The effect of the dc field is lumped into the unperturbed Hamiltonian H_o. The density matrix ρ can be expanded in powers of V as

$$\rho = \rho^{(0)} + \rho^{(1)} + \rho^{(2)} + \ldots \tag{3}$$

where $\rho^{(n)} \propto V^n$. $\rho^{(0)}$ is thus the thermal equilibrium value of ρ.

$$\rho^{(0)} \equiv \bar{\rho} = \frac{\exp\left(-\frac{H_o}{kT}\right)}{\mathrm{tr}\left[\exp\left(-\frac{H_o}{kT}\right)\right]} \quad . \tag{4}$$

In the absence of any relaxation phenomena, ρ obeys

$$\frac{\partial \rho_{ij}}{\partial t} = -i\omega_{ij} - \frac{i}{\hbar}\left[V, \rho\right]_{ij} \tag{5}$$

where $\hbar\omega_{ij} = E_i - E_j$. To include the effect of collisions we modify (5) phenomenologically to

$$\frac{\partial \rho_{ij}}{\partial t} = -i\omega_{ij} - \frac{i}{\hbar}\left[V, \rho\right]_{ij} - \gamma_{ij}\left(\rho - \bar{\rho}\right)_{ij} \tag{6}$$

so that γ_{ij} ($i \neq j$) is the rate for phase destroying collisions due to elastic and inelastic collisions. γ_{ii} is the inverse of the lifetime of level i.

Using (3) in (6) gives

$$\frac{\partial \rho_{ij}^{(n)}}{\partial t} = -\left(i\omega_{ij} + \gamma_{ij}\right)\rho_{ij}^{(n)} - \frac{i}{\hbar}\left[V, \rho^{(n-1)}\right]_{ij}$$

whose formal solution is

$$\rho_{ij}^{(n)}(t) = -\frac{i}{\hbar}\int_{-\infty}^{t} dt' e^{i(\omega_{ij} - i\gamma_{ij})(t' - t)}\left[V(t'), \rho^{(n-1)}(t')\right]_{ij} . \tag{7}$$

We solve (7) for the case when

$$\bar{E}(t) = \frac{\bar{E}_3}{2} e^{i\omega_3 t} + \frac{\bar{E}_2}{2} e^{i\omega_2 t} + \text{c.c.} \tag{8}$$

The desired mixing term at $\omega_1 = \omega_3 - \omega_2$ results in lowest order from $\rho^{(2)}$ in (1); i.e.,

$$P_\alpha^{(2)} = N\,\mathrm{tr}\left[\rho^{(2)}\mu_\alpha\right] \tag{9}$$

so that two iterations of (7) are necessary.

Anticipating the result, we keep only resonant terms (i.e., those with nearly vanishing denominators) and take $\overline{\rho}_{33} = 0$ obtaining

$$\rho_{13}^{(1)} = -\frac{i}{2\hbar}\frac{\overline{\rho}_{11}\mu_{13}E_3}{[i(\omega_{31} - \omega_3) - \gamma_{13}]} e^{i\omega_3 t}$$

$$\rho_{12}^{(1)} = \frac{i}{2\hbar}\frac{(\overline{\rho}_{22} - \overline{\rho}_{11})\mu_{12}E_2}{[i(\omega_{21} - \omega_2) - \gamma_{12}]} e^{i\omega_2 t}$$

which are used in (7) and (9) to give

$$P_\alpha^{(2)} = \rho_{23}^{(2)}(\mu_\alpha)_{32} + \rho_{32}^{(2)}(\mu_\alpha)_{23}$$

$$= \frac{1}{4\hbar^2}\left\{\frac{N_1\mu_{12}\mu_{13}(\mu_\alpha)_{32}}{[\gamma_{13} + i(\omega_3 - \omega_{31})][\gamma_{32} - i(\omega_{32} - \omega_1)]}\right.$$

$$\left. - \frac{(N_2 - N_1)\mu_{12}\mu_{13}(\mu_\alpha)_{32}}{[\gamma_{12} - i(\omega_2 - \omega_{21})][\gamma_{32} - i(\omega_{32} - \omega_1)]}\right\} E_3 E_2^* e^{i\omega_1 t}$$

$$+ \text{c.c} \qquad (10)$$

In the language of nonlinear optics[5] we characterize the optical mixing by a parameter

$$d_{\alpha 32}^{\omega_1 = \omega_3 - \omega_2}$$

defined by

$$P_\alpha^{\omega_1 = \omega_3 - \omega_2} = \frac{1}{2} d_{\alpha 32}^{\omega_1 = \omega_3 - \omega_2} E_3 E_2^* e^{i(\omega_3 - \omega_2)t}$$

$$+ \text{complex conj.} \qquad (11)$$

so that from (10)

$$d_{\alpha 32}^{\omega_1 = \omega_3 - \omega_2} = \frac{1}{2\hbar^2} \left[\frac{N_1 \mu_{12} \mu_{13} (\mu_\alpha)_{32}}{[\gamma_{13} + i(\omega_3 - \omega_{31})][\gamma_{32} - i(\omega_{32} - \omega_1)]} \right.$$

$$\left. - \frac{(N_2 - N_1) \mu_{12} \mu_{13} (\mu_\alpha)_{32}}{[\gamma_{12} - i(\omega_2 - \omega_{21})][\gamma_{32} - i(\omega_{32} - \omega_1)]} \right] . \qquad (12)$$

This is our basic result, valid for a homogeneously broadened transition. In the following section we will integrate it over the doppler distribution to derive the nonlinear coefficients for a gas exhibiting simultaneous pressure and doppler broadening.

C. Pressure Dependence and Dispersion

The expression for $d^{\omega_1 = \omega_3 - \omega_2}$ given above assumed operation in the pressure broadened region where doppler broadening is negligible. For optimization of the nonlinear coefficient it will be important to understand in detail the transition region and the pressure dependence of both the absorption (γ) and the nonlinear coefficients. The behavior of d and γ (in this region) as well as their dispersion, are also of fundamental spectroscopic importance and contain useful information about the broadening and collision mechanism.

We now allow for a velocity distribution of the gas molecules described by a Maxwellian

$$g(v) = \frac{1}{\sqrt{2\pi}\,\sigma} e^{-v^2/2\sigma^2} \tag{13}$$

so that σ is the rms velocity. Assuming perfect resonance $\omega_{31} = \omega_3$ and $\omega_{32} = \omega_1$ for stationary molecules and taking $N_1 = N_2$, $N_3 = 0$ we replace $(\omega_{32} - \omega_3)$ in (12) by $\omega_{32} v/c$ to allow for the Doppler energy shift of atoms v. Similarly, $(\omega_3 - \omega_{31}) \rightarrow - \omega_{31} v/c$. The velocity averaged $d^{\omega_1 = \omega_3 - \omega_2}$ is thus

$$d^{\omega_1 = \omega_3 - \omega_2} = - \frac{N_1 \mu_{12} \mu_{13} \mu_{32}}{2\hbar^2} \int \frac{g(v)}{\left(\frac{\omega_{32} v}{c} - i\Gamma\right)\left(\frac{\omega_{31} v}{c} - i\Gamma\right)} \, dv \tag{14}$$

where $\Gamma \equiv \gamma_{13} \simeq \gamma_{32}$ is the sum of the natural and pressure induced linewidths.

The integral occurring in (14) can be separated into sums of plasma dispersion integrals and is evaluated to be

$$\int dv = \sqrt{\frac{\pi}{2}} \frac{c}{\gamma \Gamma \omega_{21}} \left\{ F\left(\frac{c\Gamma}{\sqrt{2}\,\sigma\omega_{32}}\right) - F\left(\frac{c\Gamma}{\sqrt{2}\,\sigma\omega_{31}}\right) \right\} \tag{15}$$

$$\simeq \sqrt{\frac{\pi}{2}} \frac{c}{\sigma\omega_{31}} \frac{\partial F}{\partial \Gamma} \quad \text{for} \quad \omega_{21} << \omega_{31}, \omega_{32} \tag{16}$$

where

$\int dv$ refers to the integral in (14) and

$$F(x) = e^{x^2}\ \mathrm{erfc}(x)$$

(erfc(x) = complementary error function).

Using (16) in (14) yields

$$d^{\omega_1 = \omega_3 - \omega_2} = -\frac{N_1\mu_{12}\mu_{13}\mu_{32}}{2\hbar^2}\sqrt{\frac{\pi}{2}}\,\frac{c}{\sigma\omega_{31}}\left(\frac{\partial F}{\partial \Gamma}\right) \qquad (17)$$

We note that the argument of the F function, $c\Gamma/(\sqrt{2}\,\sigma\omega_{31})$, is the ratio of the homogeneous linewidth to the Doppler linewidth. It is essentially proportional to pressure so that eq. (17) describes the pressure dependence of the nonlinear coefficient d.

Although a numerical estimate of d based on (17) is possible, a safer procedure and one that serves a check is to relate d to the linear absorption coefficient (due to $1 \rightarrow 3$ transitions), γ. Using the same formalism and symbols we obtain

$$\gamma = \frac{4\pi\,|\mu_{13}|^2 N_1}{o\hbar}\sqrt{\frac{\pi}{2}}\,F\left(\frac{c\Gamma}{\sqrt{2}\,\sigma\omega_{31}}\right)$$

$$\equiv \gamma_H\,\sqrt{\pi}\,x e^{x^2}\,\mathrm{erfc}(x) \quad ,$$

$$x = \left(\frac{c\Gamma}{\sqrt{2}\,\sigma\omega_{31}}\right) \qquad (18)$$

so γ_H = value of γ at $x \to \infty$ (high pressure). Combining (18) with (17) yields, after some mathematical manipulation,

$$d^{\omega_1 = \omega_3 - \omega_2} = -\frac{c\mu_{12}}{8\pi\hbar\omega_{31}}\left(\frac{\mu_{23}}{\mu_{13}}\right)\sqrt{\frac{\pi}{2}}\,\frac{c\gamma_H}{\sigma\omega_{31}}\left[2x^2F(x) - \frac{2}{\sqrt{\pi}}x\right] \qquad (19)$$

Note that μ_{12} is determined precisely from the Stark splitting rate ($\Delta E_{Stark} = 2\mu_{12}E$ at high fields) $\mu_{23}/\mu_{31} \sim 1$, while γ_H is the asymptotic value of the absorption coefficient of the $1 \to 3$ transition at high pressures ($x \gg 1$).

D. Nonlinear Coefficient of NH_2D

From (12) it follows that a large nonlinear coefficient

$$d_{\alpha 32}^{\omega_1 = \omega_3 - \omega_2}$$

results when the applied photon energies of the microwave field ω_2 and the optical frequency ω_3 are nearly resonant with some transitions ω_{31} and ω_{32}.

An atomic system which meets these requirements is that of the molecule NH_2D. The relevant transitions are rotational vibrational and are shown in Fig. 3.

Levels 1 and 2 are nearly degenerate with a (zero field) splitting of 644 MHz. Their (ν_2) vibrational symmetry is indicated on the left. Level 1 is odd (antisymmetric - a) while 2 is even (symmetric - s). The application of a dc electric field causes a quasilinear Stark splitting of these two states as shown. At a field of 3570 V/cm the transition energy $\hbar\omega_{31}$ is equal to the photon energy of the P(20) CO_2 laser line at 944 cm^{-1}. At this field the $|M| = 4$ states separation is 4134 MHz (Ref. 6).

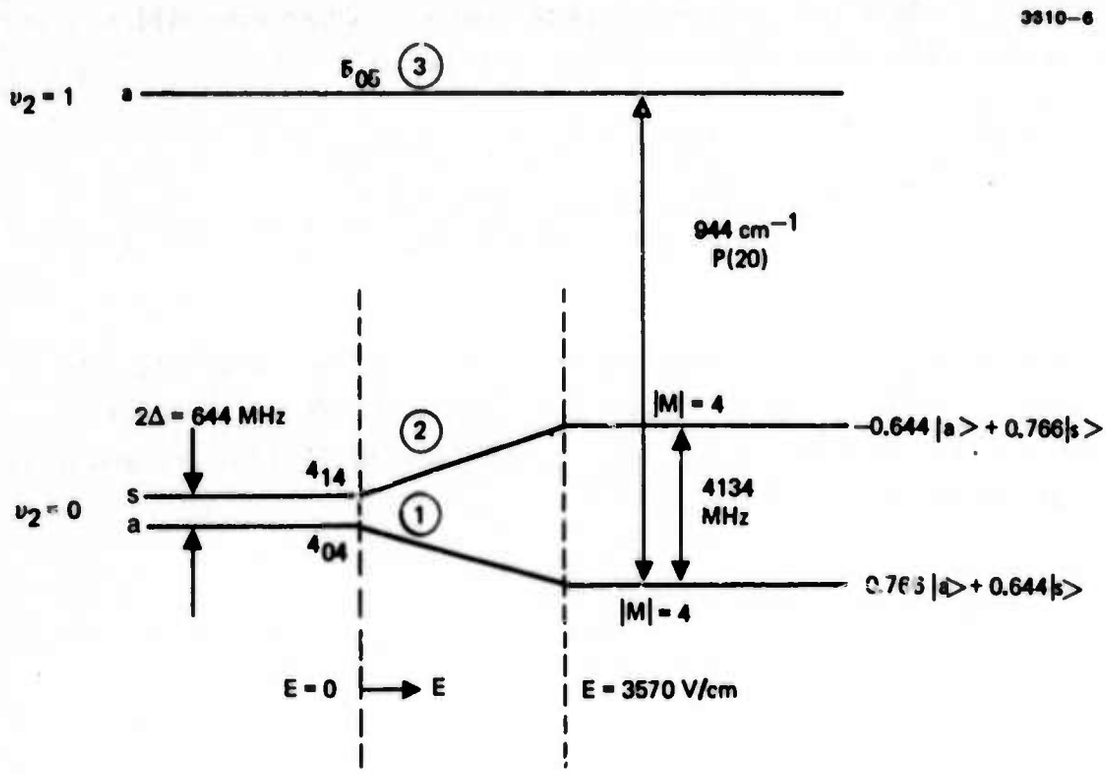

Fig. 3. Some of the energy levels relevant to the derivation of the nonlinear coefficient d_{123}.

The splitting $\hbar\omega_{21}$ is given by

$$\hbar\omega_{21} = 2\sqrt{\Delta^2 + \mu_{ab}{}^2 E^2} \tag{20}$$

where μ_{ab}, the dipole matrix element connecting level 1 and 2, is accurately determined from Stark effect measurements[6] to be $\mu_{ab} = 1.14 \times 10^{-18}$ esu.

The applied dc field causes an admixture of states 1 and 2. This admixture is crucial. Without it the dipole matrix element $\langle 1|\mu|3\rangle = \langle a|\mu|a\rangle = 0$ by symmetry. It follows from (12) that the nonlinear coefficient is zero. In the presence of a field the vibrational symmetry is destroyed and

$$\begin{aligned} |2\rangle &= -a_1|a\rangle + a_2|s\rangle \\ |1\rangle &= a_2|a\rangle + a_1|s\rangle \end{aligned} \tag{21}$$

where

$$\frac{a_2}{a_1} = \frac{\Delta}{\mu_{ab}E} + \sqrt{1 + \frac{\Delta^2}{\mu_{ab}{}^2 E^2}} \quad . \tag{22}$$

It follows that the dipole matrix element μ_{12} which enters into the expression (12) for d is

$$\mu_{12} = \left(a_2{}^2 - a_1{}^2\right)\mu_{ab} \tag{23}$$

At an applied field of 3570 V/cm, needed to resonate the P(20) CO_2 laser line, we have from (15)

$$|2\rangle = -0.644|a\rangle + 0.766|s\rangle$$

$$|1\rangle = 0.766|a\rangle + 0.644|s\rangle \qquad (24)$$

and

$$\mu_{12} = \mu_{ab}(0.586 - 0.414)$$

$$= 0.174\mu_{ab} = 0.198 \times 10^{-18} \text{ esu} \quad . \qquad (25)$$

Equation 19 relates the nonlinear coefficient to the experimentally measured[3] high pressure value of the linear absorption coefficient. Although it is possible to relate the nonlinear coefficient directly to the dipole matrix elements (see eq. 17), the uncertainties in estimating the percent concentration of NH_2D in the mixture as well as the partition function for level 1 are such that it is more reasonable to use the measured absorption directly. In this way, the NH_2D concentration and partition function are automatically included. From the data of Ref. 3, we estimate for a 50:50 ND_3 - NH_3 mixture,

$$\gamma_H = 0.042 \text{ cm}^{-1} \qquad (26)$$

$$\Gamma/P = 2\pi\,(32 \text{ MHz/Torr}) \qquad (27)$$

From eq. 29, inserting $\sigma = \sqrt{RT/m}$, μ_{12}, and the laser frequency ω_{31} into eq. 19, we have

$$d^{\omega_1 = \omega_3 - \omega_2} = 8.27 \times 10^{-6}\, \gamma_H\, G(x)$$

$$= 3.47 \times 10^{-7}\, G(x) \text{ esu} \qquad (29)$$

where γ_H is in cm^{-1}, and G(x) is dimensionless, defined as

$$G(x) = 2x\left[\frac{1}{\sqrt{\pi}} - x\, e^{x^2}\ \mathrm{erfc}\,(x)\right] \tag{30}$$

$$x = \frac{c\Gamma}{\sqrt{2}\,\sigma\omega_{31}} = \frac{\text{Pressure Broadened Linewidth}}{\text{Doppler Linewidth}} \quad . \tag{31}$$

The function G(x) versus x, and equivalently d versus pressure for NH_2D, are shown in Fig. 4. The peak value for the nonlinear coefficient occurs at ~1.2 Torr and has a value

$$d^{\omega_1 = \omega_3 - \omega_2} = 9.6 \times 10^{-8}\ \text{esu} \tag{32}$$

The coefficient d estimated above refers to the generation of a sideband at ω_1 by mixing a CO_2 P(20) line with a microwave field ω_2 (at 4134 MHz). It is appropriate to compare it to the electro-optic coefficient r_{14} of GaAs which can be used, alternatively, to generate the sideband by conventional electro-optic modulation.

Using the correspondence[7]

$$r_{jlk} = -\frac{2\epsilon_o}{\epsilon_j \epsilon_l} d_{jkl} \tag{33}$$

we have

$$\frac{(n^3 r)_{NH_2D}}{(n^3 r)_{GaAs}} \sim 1.1 \quad . \tag{34}$$

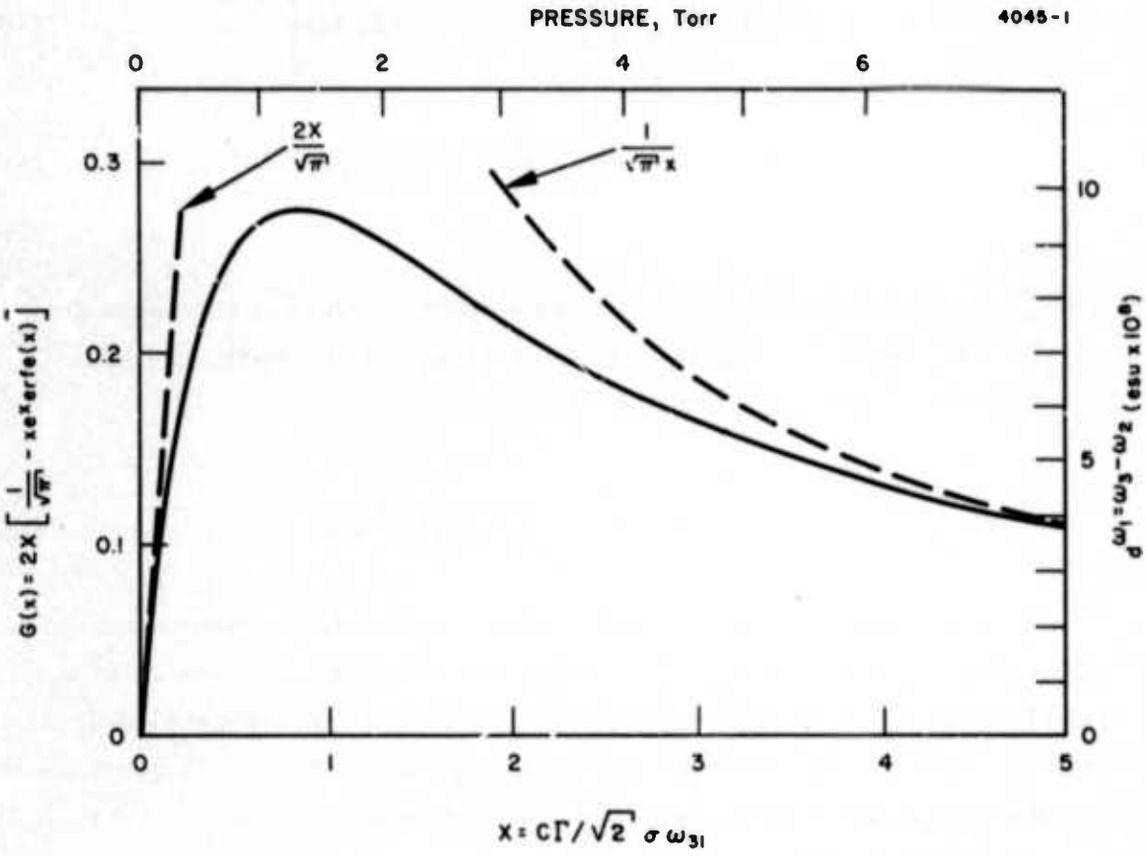

Fig. 4. Dependence of NH_2D nonlinear coefficient on pressure for exact resonance. Equivalently, the functional form of G(x) is shown.

We reach the conclusion that as far as sideband generation, dc biased NH_2D is comparable to GaAs (which is one of the best infrared modulation materials). We must recognize, however, that this large coefficient was obtained by exploiting the resonant nature of the effect. The penalty we pay is that of reduced bandwidth. In the following section, we consider the frequency response of the nonlinear coefficient.

E. Dispersion of the Nonlinear Coefficients

The treatment up to this point assumed that the applied frequencies ω_3 and ω_2 were exactly equal to the center frequencies of the respective transitions. This results, as shown above, in real nonlinear coefficients, d. If one allows a frequency deviation $\omega_3 - \omega_{31}^{(0)} \neq 0$, d is complex. The analysis is involved and will be reported in full in the final report. We find that the Im(d) is considerably larger than the real part and, moreover, occurs at the wings of the absorption. Some detailed plots of the predicted behavior are shown in Fig. 5. This indicates that the estimate of d given in the previous section is possibly conservative, and more importantly, a considerable increase in operating bandwidth may be possible by exploiting the imaginary part.

F. Frequency Conversion

One important class of applications of the dc induced optical nonlinearity is that of converting from ω_3, which in our case corresponds to the P(20) CO_2 laser line, to $\omega_1 = \omega_3 - \omega_2$ where ω_2 is the microwave frequency at 4134 MHz. Here we estimate the percentage of ω_3 input power which we may expect to down-convert under realizable circumstances.

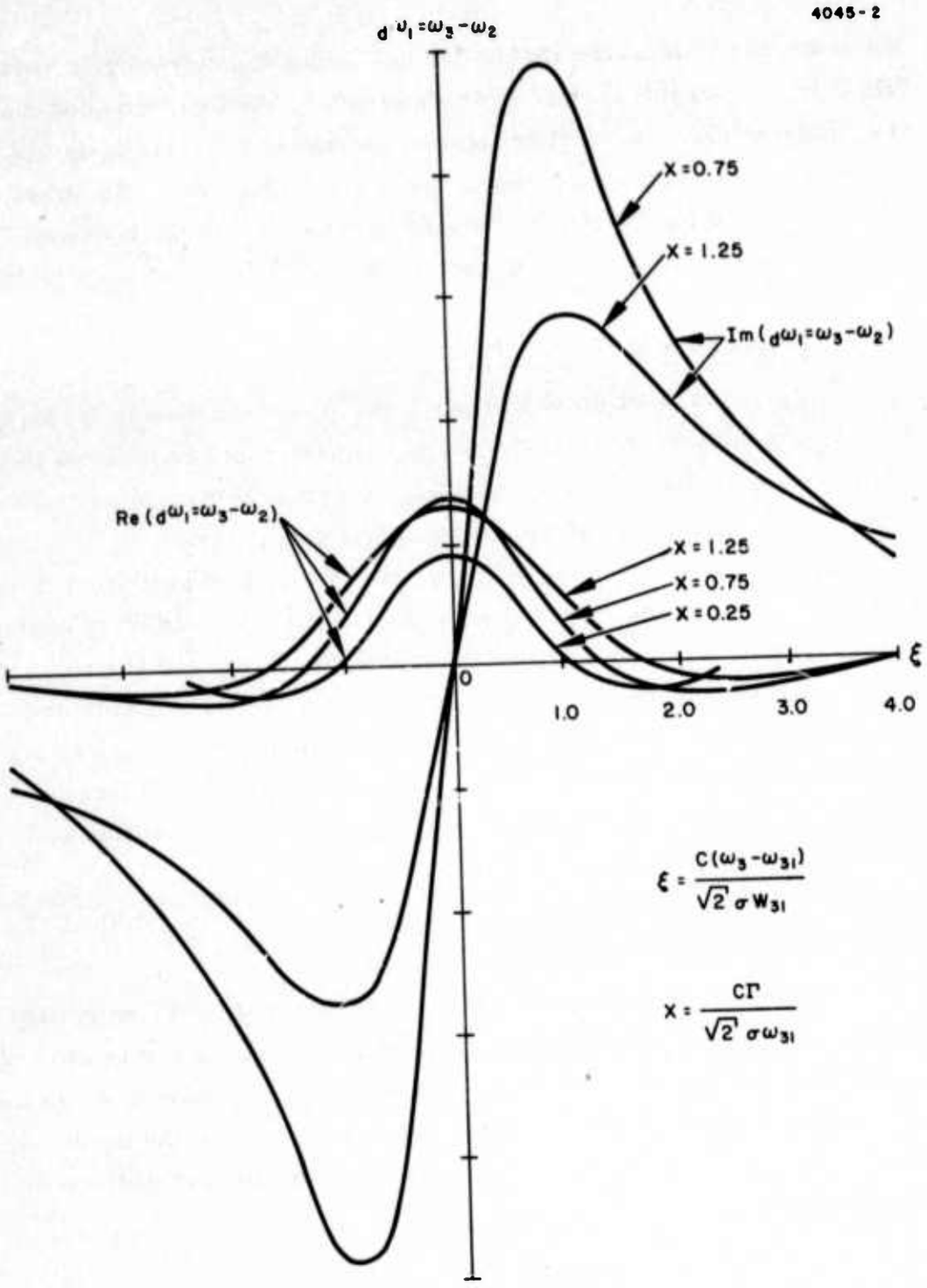

Fig. 5. The dependence of the real and imaginary parts of the mixing constant d on detuning (pressure is a parameter).

If we neglect the effects of absorption, the relevant differential equations for the field amplitudes A_1 and A_3 are[7]

$$\frac{dA_1}{dx} = -i \frac{g}{2} A_3 e^{-i\Delta kx}$$

$$\frac{dA_3}{dx} = -i \frac{g}{2} A_1 e^{i\Delta kx} \qquad (35)$$

where

$$A_i = \sqrt{\frac{n_i}{\omega_i}} E_i \quad ,$$

$$g = \sqrt{\frac{\mu_o}{\epsilon_o} \frac{\omega_1 \omega_3}{n_1 n_3}} d_{yyz}^{\omega_1 = \omega_3 - \omega_2} E_2$$

$$\Delta k = k_3 - (k_1 + k_2) \quad . \qquad (36)$$

Assuming a single input $A_3(0)$ at $x = 0$ and phase matched operation ($\Delta k = 0$), the solution of (36) is

$$A_1(x) = -iA_3(0) \sin\left(\frac{gx}{2}\right)$$

$$A_3(x) = A_3(0) \cos\left(\frac{gx}{2}\right) \qquad (37)$$

so that a complete transfer of the input power at ω_3 to an output at ω_1 is effected in a distance π/g.

To estimate g we use the following set of conditions:

$$E_2 \sim 4 \times 10^4 \frac{V}{m} \quad . \tag{38}$$

This value is based on a microwave cavity design with a Q of 100 and an input power $P_2 = 1$ W.

$$d_{yyz} = 3.55 \times 10^{-22} \text{ MKS}$$

$$\omega_3 = 1.779 \times 10^{14} \ (= 944 \text{ cm}^{-1}) \quad . \tag{39}$$

The result is

$$g = 0.01 \text{ cm}^{-1}$$

so that a complete power transfer from ω_3 to ω_1 will require an interaction path of $\pi/g \sim 314$ cm. However, as can be seen in Fig. 5, off resonance operation is expected to result in a factor of ~ 3.5 improvement in this value, and will also reduce the effects of linear absorption on the conversion process.

III. EXPERIMENTAL PROGRESS

The experimental portion of the program has been directed toward the design and construction of an rf excited Stark device along with the construction and testing of specialized equipment that will be required to perform the parametric mixing experiments. We have constructed a number of coaxial monitor tees and impedance transformers for matching our 50 Ω test equipment to the generally higher impedance Stark devices and have purchased a 2 to 5 GHz voltage controlled oscillator (VCO). The VCO has been packaged with associated power supplies into a fast tuning rate sweep signal generator that can be frequency modulated at rates up to 50 MHz. A traveling wave tube (TWT) amplifier has been obtained that will allow the 100 mW signals from the VCO to be amplified to 10 W between 2 and 4.5 GHz. A number of rf power meters, low level amplifiers, frequency meters and a spectrum analyzer have also been set up. Testing and calibration of the fabricated rf equipment has been completed.

We have been conducting radio frequency Stark experiments using standard Stark cells designed and built at Hughes, and several new transmission line structures that are being fabricated for this program. The conventional devices have 10 cm long evaporated gold electrodes on alumina blocks spaced 1.2 mm apart. The blocks are enclosed in a steel can and the electrodes are coaxially fed. The alumina blocks provide excellent arc suspension to kilovolt potentials. Figure 6 shows the stainless steel cylinder which encloses the alumina structure shown in the foreground. The triple stub tuner attached to the feed line was designed to enable us to resonate the device at 4 GHz. The Stark voltages for various CO_2 laser transitions range between 300 and 500 V. A series of rf experiments has been conducted using the alumina cells and frequency modulation of the Stark resonance has been demonstrated between dc and 100 MHz by applying dc and rf energy to opposing electrodes. Above 50 MHz spurious rf pickup by the sensitive receiver equipment has become a problem. Fortunately the lower

M10916

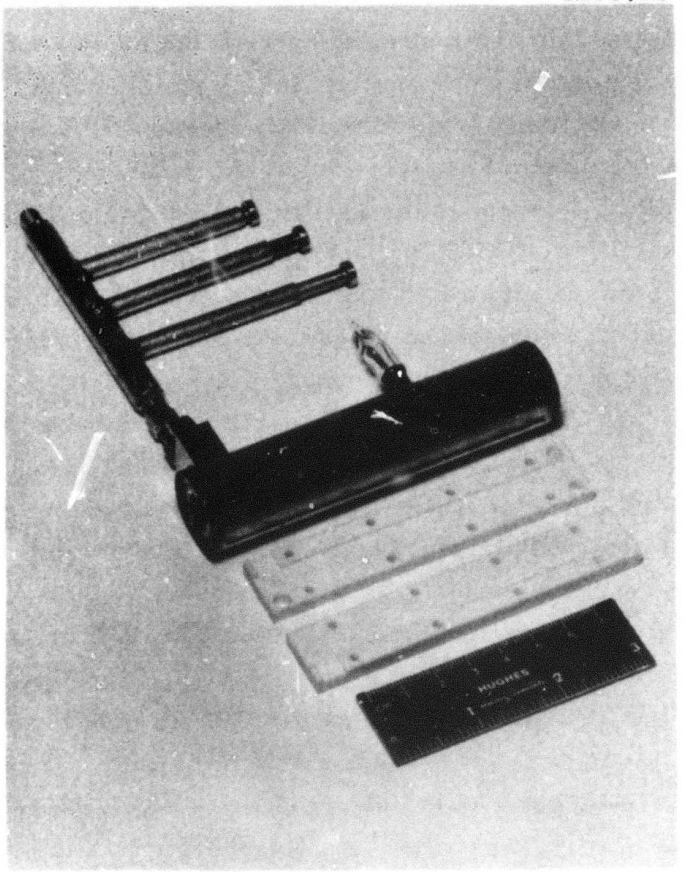

Fig. 6. Conventional Stark cell with 3 stub microwave tuning assembly attached. Alumina electrode structure shown in foreground.

M10915

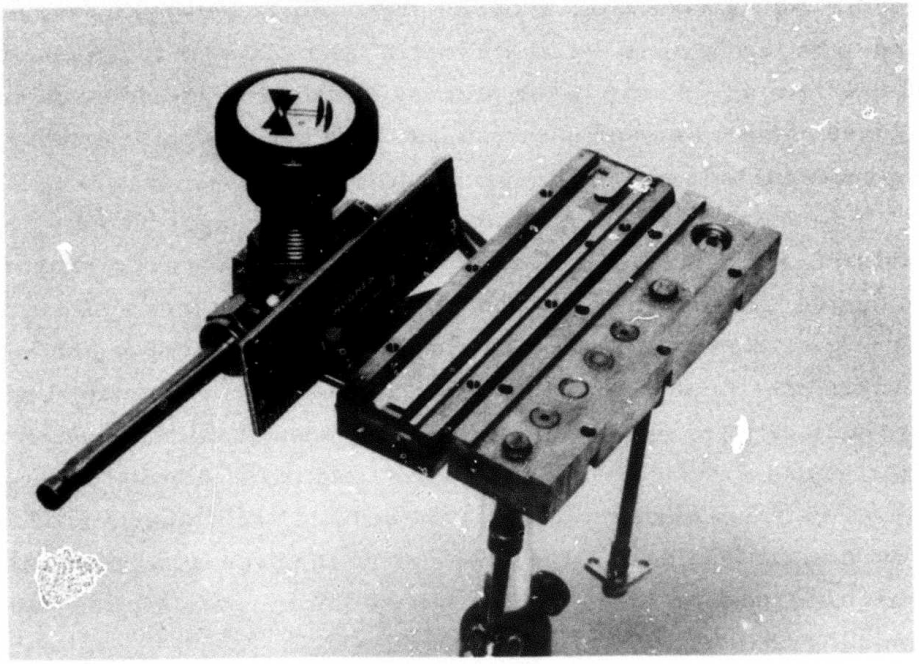

Fig. 7. Triplate microwave Stark cell with top removed showing microwave coupling and tuning probes and type BNC dc bias connector.

frequency fm experiments have utilized the same equipment we plan to use for the 4 GHz experiments. Optical modulation experiments at rates up to 100 MHz have disclosed which components are susceptible to radio frequency interference (RFI). In particular the SAT HgCdTe detector and its associated bias and preamplifier networks have been found to be highly sensitive to RFI when the modulator is driven at only 100 mW levels. We are in the process of shielding the detector and receiver components and have relocated the experiment in a laboratory less susceptible to external sources of RFI.

A series of 4 GHz measurements have been conducted by resonating air filled windowless alumina Stark devices in a short circuit terminated transmission line configuration. A high loss aquadag bead on a nylon string was then pulled through the interaction region between the electrodes to perturb the rf fields. Input impedance matching combinations were found which produced loaded Q values between 20 and 50 for modes which contain some of the field in the interaction region. Several spurious modes were encountered and are probably produced by the coaxial feed design. We are now in the process of modifying the connectors and feed wires to improve the microwave coupling into the alumina structure.

Several dummy and two operating triplate resonator devices similar to those discussed in our original proposal have been constructed. Figure 7 shows a triplate device with the microwave coupling circuitry removed and laying in the foreground. The glass card and Irtran end windows confine the NH_3 gas, while the microwave coupling probes, tuning slugs and dc feed can be removed without opening the gas cell to air. These devices have 5 mm x 100 mm gold electrodes evaporated on both sides of the glass slide and a dc block can be seen at the far end of the structure as a gap in the gold film. In operation, a microwave shorting bar is placed across the glass in front of the dc block to confine the rf energy to the forward part of the structure. Q values as high as 250 have been measured at 4.1 GHz with coupling coefficients close to unity. The devices can be tuned ±40 MHz with capacitive plungers or several GHz with a sliding microwave short

circuit. Figure 8 shows the power coupled through the triplate structure at resonance as a function of frequency and capacitive tuning.

Probing the fields as a function of position in the Stark interaction region showed the velocity of propagation to be about 0.8 c. Measurements at dc with NH_3 in the device were made, and the Stark resonance amplitude was about 6% of the 10.6 μm energy as compared with 11 to 14% for the more rigid alumina device. Radio frequency measurements at 100 MHz gave no optical modulation as had been detected with the alumina device. We found that the longer wavelength rf energy (i.e., $\lambda > 20$ cm) was not coupling through the glass to the electrode inside the Stark cell. The long wavelength energy was confined in the top section of the triplate in a strip line type mode. This result was unfortunate for it would be desirable to tune and align the equipment at 100 MHz before undertaking the more elaborate 4.1 GHz experiments. We believe we can force the fields below 100 MHz into the Stark cell by removing the top plate of the structure; however, this produces severe rf radiation into the laboratory and the stray pickup saturates our present receiver configuration.

During the next reporting period we first plan to complete the rf shielding required to eliminate stray rf pickup when operating at full low driver power levels. If necessary, we can also spatially isolate the optical detector and receiver by passing the laser beam between adjacent laboratories. At the same time we will complete the rf feed redesign for the alumina devices and will also continue to refine the triplate structure in an attempt to force the longer rf fields into the Stark interaction region. Our design goal is to combine the high rf efficiency of the triplate device at 4 GHz with the high Stark efficiency and arc suppression of the alumina device. With this optimum structure we will perform 4 GHz mixing experiments.

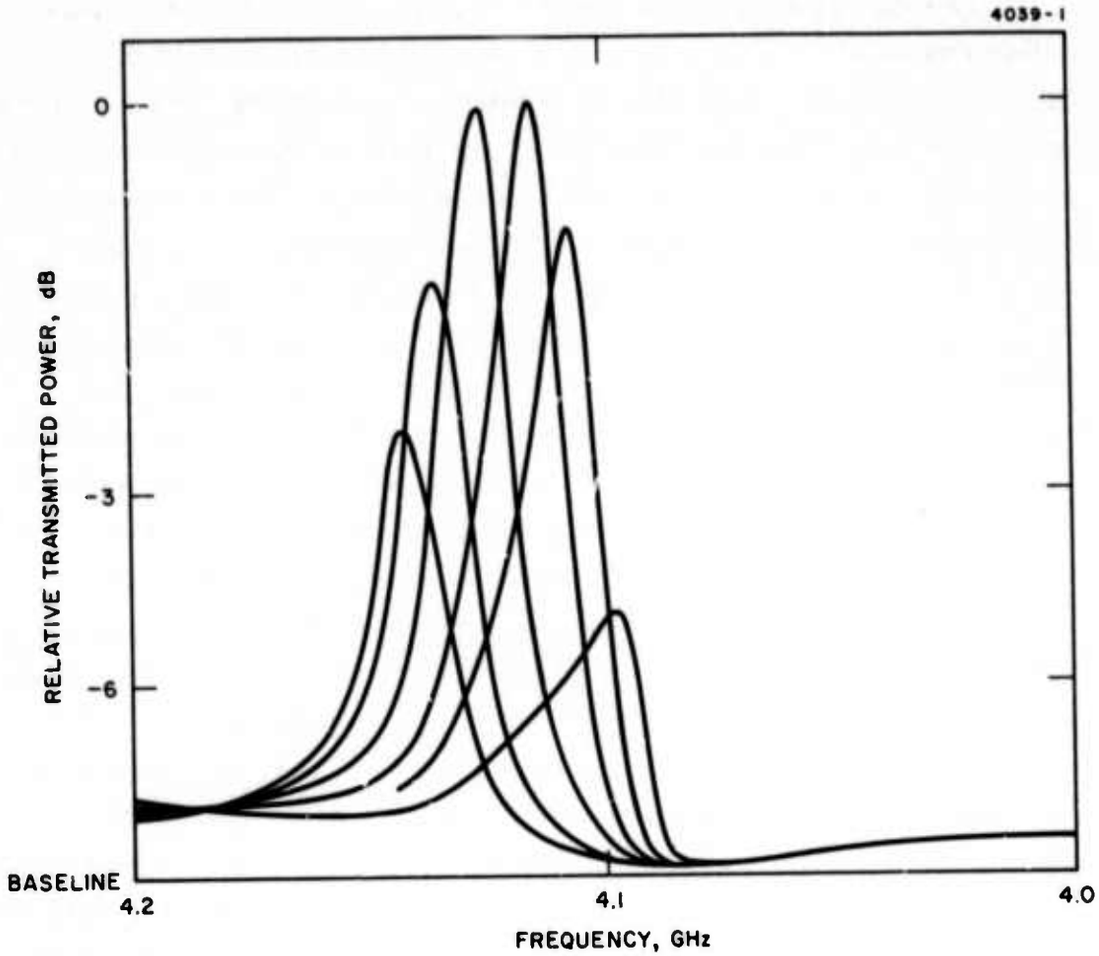

Fig. 8. Triplate resonator tuning as a function of capacitive loading Q ≈ 250.

REFERENCES

1. R. G. Brewer, M. J. Kelly, and A. Javan, Phys. Rev. Lett. 23, 559 (1969).

2. M. J. Kelly, R. E. Francke, and M. S. Feld, J. Chem. Phys. 53, 2979 (1970).

3. A. R. Johnston and R. D. S. Melville, Jr., Appl. Phys. Lett. 19, 503 (1971).

4. R. L. Abrams, Appl. Phys. Lett. 25, 304 (1974).

5. See, for example, N. Bloembergen, Nonlinear Optics, W. Benjamin, New York, 1962.

6. T. A. Nussmeier and R. L. Abrams, Appl. Phys. Lett. 25, 615 (1974).

7. A. Yariv, Introduction to Optical Electronics, Holt Rinehart and Winston, New York, 1972.